J Mol Model (2013) 19:3271–3278
DOI 10.1007/s00894-013-1854-4

ORIGINAL PAPER

Metal ions in sugar binding, sugar specificity and structural stability of *Spatholobus parviflorus* seed lectin

Joseph Abhilash · Kalarickal Vijayan Dileep · Muthusamy Palanimuthu · Krishnan Geethanandan · Chittalakkotu Sadasivan · Madhathilkovilakath Haridas

Received: 28 November 2012 / Accepted: 16 April 2013 / Published online: 8 May 2013

Abstract *Spatholobus parviflorus* seed lectin (SPL) is a heterotetrameric lectin, with two α and two β monomers. In the crystal structure of SPL α monomer, two residues at positions 240 and 241 are missing. This region was modeled based on the positional and sequence similarities. The role of metal ions in SPL structure was analyzed by 10 ns molecular dynamics simulation. MD simulations were performed in the presence and absence of metal ions to explain the loss of haemagglutinating property of the lectin due to demetallization. Demetallized structure was found to deviate drastically at the metal binding loop region. Affinity of different sugars like N-acetyl galactosamine (GalNAc), D-galactose and lactose towards the native and demetallized protein was calculated by molecular docking studies. It was found that the sugar binding site got severely distorted in demetallized lectin. Consequently, sugar binding ability of lectin might be decreasing in the demetallized condition. Isothermal titration calorimetric (ITC) analysis of the sugars in the presence of native and demetallized protein confirmed the *in silico* results. It was observed after molecular dynamics simulations, that significant structural deviations were not caused in the quaternary structure of demetallized lectin. It was confirmed that the structural changes modified the sugar binding ability, as well as sugar specificity of the present lectin. The role of metal ions in sugar binding is described based on the *in silico* studies and ITC analysis. A comprehensive analysis of the ITC data suggests that the sugar specificity of the metal bound lectin and the loss of sugar specificity due to metal chelation are not linear.

Keywords SPL · Demetallization · Glide docking · Molecular dynamics

J. Abhilash and K. V. Dileep equally contributed.

J. Abhilash · K. V. Dileep · M. Palanimuthu · K. Geethanandan · C. Sadasivan · M. Haridas (✉)
Department of Biotechnology & Microbiology and Inter-University Centre for Bioscience, Kannur University, Thalassery Campus, Palayad 670661, India
e-mail: mharidasm@rediffmail.com

Present Address:
K. Geethanandan
Molecular Biophysics Unit, Indian Institute of Science, Bangalore 560 012, India

Introduction

Lectins are multivalent carbohydrate-binding proteins. The biological properties of lectins are mediated through their ability to bind specifically with different sugars [1–7]. Lectins were first identified in plants and their best-characterized property was the ability to agglutinate red blood cells. So, lectins are referred to as phytohaemagglutinins. Subsequently, lectins have been identified and characterized in other forms of life such as animals, bacteria, fungi and viruses [7, 8]. The importance of carbohydrate as the energy source and its crucial role in maintaining the structural integrity of plants has long been recognized. The role played by carbohydrates in biological recognition has become an important area of research recently [8]. It turns out that a substantial part of the recognition events, particularly on cell surfaces, are mediated through specific interactions between proteins and diverse carbohydrate structures. On the tumor cell surface, lectins interact with specific carbohydrate structures. This property of lectins is exploited to discriminate malignant from normal cells [9]. For this reason and indeed for the insights they provide to the structural diversity of proteins and the strategies for generating ligand specificity, lectins have been received with considerable attention.

Spatholobus parviflorus seed lectin (SPL) is a hetero dimeric tetramer lectin, with two α and two β monomers forming the tetramer. α chain consists of 251 and β chain

consists of 239 amino acid residues. In α chain, the residues 240 and 241 were not found due to the poor electron density. So, they were designated as 'unknown' (xx) [10] in its sequence. Sequence similarity revealed that SPL belongs to the legume lectin family. The secondary structure consists of 6 % α helices (4 helices; 17 residues) and 42 % beta sheets (20 strands; 106 residues). A little over 50 % of the residues form the loops connecting these sheets or the strands in them. The 18 β strands of SPL form a jelly roll like structure as in the other legume lectins. The jelly roll model consists of anti-parallel six stranded β-sheet, curved seven stranded front β-sheet and a short five member β-sheet as a cap to the molecule. The sheets are connected by many loops [11]. Dimers/tetramers are stabilized by the hydrogen bonds formed between the monomers.

Biochemical studies revealed that SPL is a galactose specific lectin [10]. Sugar binding pocket in SPL consists of the residues D88, G106, Y130, N132, T133, G217 and A218. There are two metal ions in each monomer, one each of Ca^{2+} and Mn^{2+}. They were confirmed by atomic absorption spectrophotometry and could be removed by the chelating agents like EDTA. Structure analysis reveals that the metal coordination is through the residues E126, D128, Y130, N132, D137 and H142. The sugar and metal binding sites are found to be conserved in legume lectins. Two residues, Y130 and N132, are involved in both sugars binding as well as metal binding. For analyzing the structural similarity, SPL was compared with some of the legume lectins and showed more that 60 % sequence similarity [12–15].

Among the computational approaches to study and explore biological systems at atomic level, molecular dynamic (MD) simulations are found to be applied successfully for a number of biological macromolecules. MD simulations have been used to study different lectins like Peanut agglutinin (PNA), Concanavalin A (ConA), *Erythrina corallodendron* lectin (EcorL) [16–19] and their different sugar complexes. These studies demonstrated MD as a complementary method to crystallography and other experimental methods which gave insight to the structure [20]. The present MD study focuses on the role of metal ions in the sugar binding and quaternary structural assembly of SPL.

Materials and methods

Metal ions in hemagglutination

Demetallization and hemagglutination assay of SPL

SPL was demetallized by dialyzing against 0.58 mM of EDTA in phosphate buffer of pH 7.4 for 72 h. After demetallization, the protein solution was dialyzed for 72 h against phosphate buffer of same pH to remove EDTA. Both the native and demetallized proteins were tested for hemagglutination of human red blood cells (RBCs), prepared in phosphate buffer in physiological saline. The two proteins were serially diluted on a microtitre plate and checked for hemagglutination activity.

Simulation studies

Modeling of missing residues in α monomer

In order to model the missing regions of α chain, BLAST analysis was carried out to identify the related sequences. As a result of BLAST analysis, 156 similar lectin sequences were collected from the non redundant database and these sequences were aligned together using Clustal X [21]. It was observed that all the collected sequences were aligned perfectly to α chain of SPL and the minimum alignment score obtained was 89 %. The signature was constructed for the missing residues based on the frequency of amino acids at the corresponding positions.

Preparation of the protein structure

The modeled protein was prepared using protein preparation wizard of Schrödinger Maestro 9.1. Polar hydrogens were added and bond orders were assigned properly. The metals were treated and coordination was corrected properly. The structure was then minimized using Impref minimization in Schrödinger Maestro 9.1. RMSD cut off of 0.30 Å was applied during minimization process in order to avoid the huge structural changes.

Molecular dynamics

Molecular dynamics (MD) simulations were carried out using AMBER 94 force field in the Macromodel module of Schrödinger Maestro 9.1 [22] at a temperature of 300 K. MD was applied to the native and demetallized structures. The van der Waals, electrostatic and H-bonds cut off were set at 12, 20 and 4 Å respectively. The simulations were carried out using an explicit solvent system with a water box consisting of TIP3P [23] water molecules. The water boxes used for the monomeric and tetrameric units were 50 $Å^3$ and 110 $Å^3$ respectively. The simulations were carried out both in the presence and absence of metal ions, and for the monomeric and tetrameric units of the protein. The system was energy minimized with 500 iterations of Polak-Ribiere conjugate gradient minimization (PRCG) and molecular dynamics was performed for 10 ns. A time step of 1 ps and equilibration time of 100 ps were used in all simulations.

Molecular docking

In order to identify the binding of different sugars, an induced fit docking (IFD) was carried out against native and demetallized structures (chains A and B) after molecular

dynamics (DSAMD). Docking simulations were done by (Schrödinger) Maestro 9.1. The final energy minimized structure after incorporating the missing residues was taken for the docking studies. The sugars such as N-acetyl galactosamine (GalNAc), D-galactose and lactose were prepared using Ligprep module and the prepared structures were docked into the binding site of both proteins by extra precision (XP) method.

The IFD protocol allows flexibility to both the ligand and the target. Residues D88, G106, Y130, N132, T133, G217 and A218 were used for setting the Grid. Before IFD, a constrained minimization of the receptor with an RMSD cutoff of 0.18 Å was applied. Then, initial glide docking of each ligand using van der Waals radii scaling was carried out. The best poses were retained based on the energy and the prime side-chain prediction. The minimization for each protein/ligand complex was then carried out. After that, glide redocking of each protein/ligand complex structures was carried out and the best pose selected based on the glide score.

Isothermal titration calorimetry

Of SPL 0.1 mM was prepared in 20 mM phosphate buffer, pH 7.4. 2 mM of sugars, GalNAc, D-galactose and lactose were also prepared in the same buffer. Both, protein and ligand samples were degassed before loading to the ITC machine.

The calorimetric titrations were performed at the temperature 298.15 K using VP-ITC isothermal titration calorimeter from Microcal (Northampton, MA, USA) as described in the manufacturer's instruction manual. Six μl of ligand solution was added from the rotating syringe to the cell containing protein solution. Twelve seconds time was set for each injection. A time interval of 180 s was also set between each injection to allow the exothermic peak resulting from the reaction to return to the baseline. Total 47 injections were made. The reference power was set as 10 μcal and the stirring speed was adjusted to 307 rpm. The volume of the first injection was set as 3 μl to avoid inaccuracy. The final data at the end of the injections were fitted by a nonlinear least squares method using ORIGIN software from Microcal. The binding constant (K), enthalpy change (ΔH), entropy change (ΔS) and binding free energy (ΔG) were calculated using ORIGIN software.

The ITC assay of the same sugars with demetallized protein was also done. Of demetallized protein 0.1 mM and 2 mM of sugars were prepared in phosphate buffer of pH 7.4. The parameters for ITC analysis were set as in the case of lectin with metal ions.

Results and discussion

SPL with metal ions (native protein) showed hemagglutination activity up to a dilution of 0.9×10^{-3}M, where as the demetallized protein showed hemagglutination up to 14.5×10^{-3}M dilution only, which indicated that SPL lost approximately 94 % of hemagglutinating activity due to demetallization.

From the analysis of the signatures and frequency of amino acids of SPL sequence, at the region of residues 240–241, only three amino acids were found appropriate at positions 240 (G, T and D) and 241 (T, S and N). Nine combinations were made with these residues and each combination was incorporated into the structure using protein building panel of discovery studio 2.5 [24]. In total, nine structures were constructed and these were minimized extensively by applying 25,000 steps of steepest descent and 50,000 steps of conjugate gradient using the programe Swiss PDB viewer by choosing the force field GROMOS 9643B1 [25]. Among the nine structures, lowest energy (-13910.52 kcal mol^{-1}) was observed for the structure with a combination of T and N residues at positions 240 and 241 respectively. The positions of metal ions were also energy minimized accordingly. The final energy minimized structure was used for the molecular dynamics simulation study.

In total six different MD simulations were applied to α chain, β chain and the whole structure (with all four monomers) separately in the presence and absence of the metal ions. In order to identify the structural changes after removal of metal ions, the resultant structure after MD simulation in the demetallized form (DSAMD) was superimposed to the native structure and the RMS deviations were deduced. When MD was carried out, only slight deviations were observed in the native structure. So, it was assumed that the changes occurred to DSAMD structures were due to the demetallization. The metal coordinate bonds of the metal bound residues and the corresponding deviated bonds of the demetallized residues in DSAMD structure are listed in Table 1. The super-positioning of DSAMD (orange) and native (cyan) structures of both α and β chains are depicted as Figs. 1a and b respectively. Dashed lines indicate the coordinate bonds.

In the case of α monomer, the DSAMD structure exhibited mean RMS deviation of 2.56 Å in Cα positions. The mean RMS deviations in back bone and side chain atoms were 2.60 Å and 3.37 Å respectively. In SPL, the residues at the positions 126 to 141 are considered to be forming the metal binding loop. In the native structure, Y130 and N132 of the metal binding loop make coordinate bonds with Ca^{2+} ion. Similarly, E126 and H142 make coordinate bonds with the other metal ion, Mn^{2+}. Two D residues at positions 128 and 137 make coordinate bonds with both the metal ions. It is confirmed that the orientation of metal binding loop is stabilized by nine coordinate bonds. These coordinate bonds bridge the loop to the rest of the protein structure. After 10 ns MD simulation, it was observed that the DSAMD structure was perturbed drastically as the metal binding loop was disrupted.

Table 1 The metal coordinate bonds and the metal—protein residues distances at their shifted positions in DSAMD from the metal occupied site

Residue	Atom		Distance in Å unit			
			α monomer		β monomer	
		Metal ion	Native	DSAMD	Native	DSAMD
E126	OE2	Mn^{2+}	2.1	3.9	2.4	3.0
H142	NE2	Mn^{2+}	2.2	2.7	2.2	2.7
D128	OD2	Mn^{2+}	2.1	4.3	2.1	4.9
D137	OD1	Mn^{2+}	2.3	9.9	2.3	8.1
D137	OD2	Ca^{2+}	2.3	6.9	2.6	8.7
D128	OD1	Ca^{2+}	2.4	3.7	2.5	6.3
D128	OD2	Ca^{2+}	2.6	3.1	2.7	5.3
Y130	O	Ca^{2+}	2.4	5.5	2.3	6.0
N132	OD1	Ca^{2+}	2.4	5.6	2.4	5.1

As discussed earlier, the OD1 atom of D137 made a coordinate bond with the Mn^{2+} ion at a distance of 2.3 Å. In the DSAMD structure, D137 shifted from the original position and the distance to the metal ion occupied site (D137 OD1- Mn^{2+} distance) was found to be 9.72 Å. In the similar way, the length of each coordinate bond in the native structure and the distance from the positions of the same atoms in the DSAMD structure to the metal occupied sites, were also calculated (Table 1). The NE2 atom of H142 in the DSAMD structure was deviated to 3.96 from 2.2 Å and OE1 atom of E126 was deviated from 2.1 Å to 4.6 Å from their original positions. Similarly, OD2 atom of D128 deviated to 4.05 Å from 2.1 Å (Table 1).

The residues surrounding the Ca^{2+} ion were also found to be deviated in the DSAMD structure. The OD1 and OD2 positions of the D128 were deviated by 3.6 and 5.3 Å respectively from their initial positions. In the crystal structure, the coordinate bond lengths were 2.4 and 2.6 Å respectively (Table 1). The O atom of Y130 was deviated to 5.6 Å from 2.4 Å. Similarly, the OD1 atom of N132 was deviated to 3.5 Å from 2.3 Å. The OD2 atom of D137 in the DSAMD structure was found to be deviated to 8.6 Å from 2.3 Å. The shifts in these residues have also affected the orientation of the neighboring residues (Table 1 and Fig. 1a and b). Bouckaert and co-workers determined the crystal structure of apo-concanavalin A (Con A) [26] and observed that the metal ion was required to stabilize a cis-peptide bond between A207 and D208 residues. The A87-D88 of the SPL are comparable to A207 and D208 of ConA, but the A87-D88 is not a cis-peptide bond. However, the presence

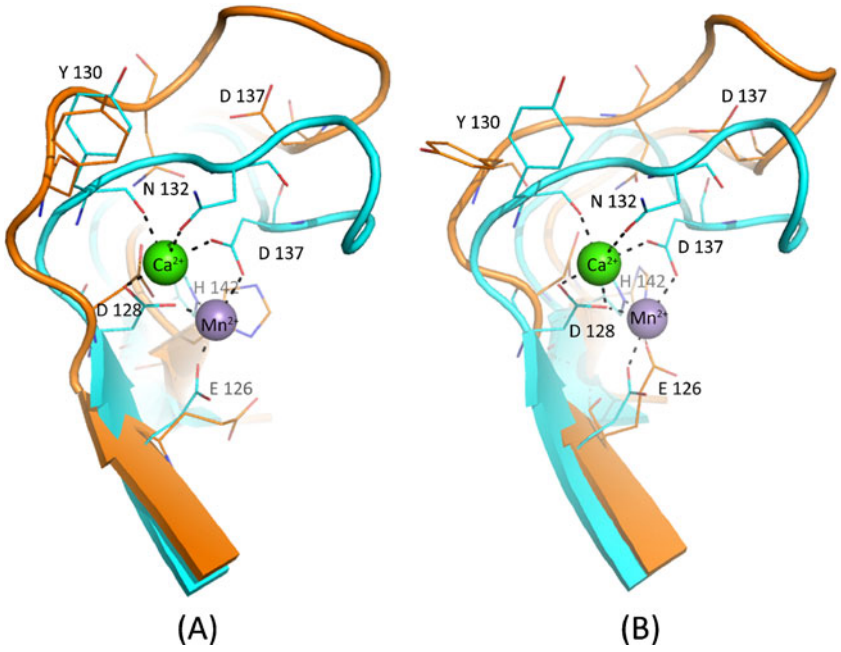

Fig. 1 The superimposition of DSAMD (*orange*) and native (*cyan*) structures of both α (**a**) and β (**b**) monomers. *Dashed lines* indicate the coordinate bonds

Table 2 Glide score of the sugar binding to the protein in the native and demetallized (DSAMD) condition

No	Sugar	Glide score in kcal mol^{-1}		
		Native	DSAMD-α	DSAMD-β
1	GalNAc	−9.37	−4.39	−4.94
2	Lactose	−8.03	−4.90	−4.59
3	D-galactose	−7.63	−4.10	−5.96

of metal ion is essential to stabilize the loop region, irrespective of the type of peptide bonds.

β chain of SPL consists of 239 residues and these are similar to α chain up to 239. Hence the metal binding regions in both chains are the same (Table 1). The DSAMD structure of β chain showed mean RMS deviation of 2.67 Å in Cα positions and 2.74 Å in backbone atoms. The side chain atoms showed 3.26 Å mean RMS deviation with respect to the native structure.

In the DSAMD structure, D137 was found to deviate from the native structure (9.9 Å) as in α chain. Similarly, O atom of Y130 and, OD1 and OD2 atoms of D128 were found to deviate by 5.5, 3.7 and 3.1 Å respectively from their original positions. Initially, the coordinate bond lengths of these residues were 2.3, 2.7 and 2.5 Å respectively. Only minor changes have been observed in the position of H142 in both the structures. In the native structure the NE2 atom of H142 was coordinately bonded with Ca^{2+} ion at a distance of 2.2 Å. It was deviated to 2.7 Å only. The other metal binding residues, such as E126, N132 were also found to deviate from the native structure. A comparative analysis showed that the deviations in α and β monomers were essentially the same.

The overall DSAMD structure (with four monomers) was also superimposed with the native structure and found to have a mean RMS deviation of 2.03 Å in Cα positions. It was noted that the loop regions in the surface of SPL deviated more compared to the rest of the structure and backbone atoms of the DSAMD structure deviated negligibly. No dissociation was observed for the tetramer of heterodimers during the 10 ns simulation. It was confirmed by the present analyses that the metal ions do not contribute to the stability of the quaternary structure of SPL.

Other loop regions (from 37 to 42 and 100 to 115) were also found to deviate drastically from their original positions. These loops were located on the surface of the protein and hence, they could move freely in the solvents.

According to the IFD results, GalNAc showed highest (−9.37 kcal mol^{-1}) glide score (Table 2). Lactose and D-galactose showed glide scores −8.03 and −7.63 kcal mol^{-1} toward α chain of the native structure. No significant difference was observed in the glide scores when sugar was bound to β chain. It was found that D88 made a similar hydrogen bond with all sugars upon binding. The same sugars were also docked into the binding region of the DSAMD structure and found that the glide scores were found to be decreased significantly. The glide scores of sugar complexes with native α and β monomers are shown in Table 2. It was also noted that in the DSAMD structure, the residue D88 could not make any hydrogen bond with the ligands as it deviated from its original position. From the super-positioning analyses it was deduced that the residue D88 was deviated by 1.65 Å from its original position. It was already reported in similar structures, that the residues such as D88, G106, Y130, N132, T133, G217 and A218 were important for sugar binding. The shifts of these residues due to the metal chelation affected the binding of sugars to the lectin. In the DSAMD structure, all these residues were deviated by at least 1.35 Å. So, it was confirmed that the structural changes affected the sugar binding ability as well as sugar specificity of lectin.

Three dimensionally, the sugar binding region of SPL resembled a 'v' shaped pot in cross section. The binding of sugar was in such a manner that it was arranged in the middle of the pot, as it had more interactions with the amino acid residues forming the cavity. It was found that the

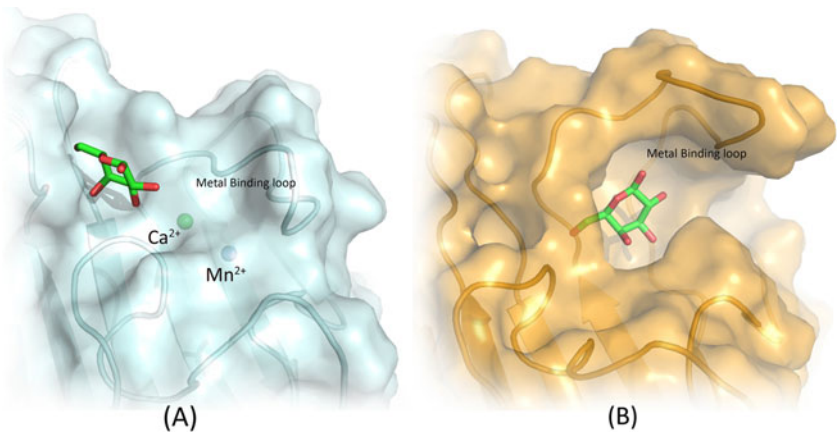

Fig. 2 Binding pattern of D-galactose in the binding pocket of both native (**a**) and DSAMD (**b**) structures

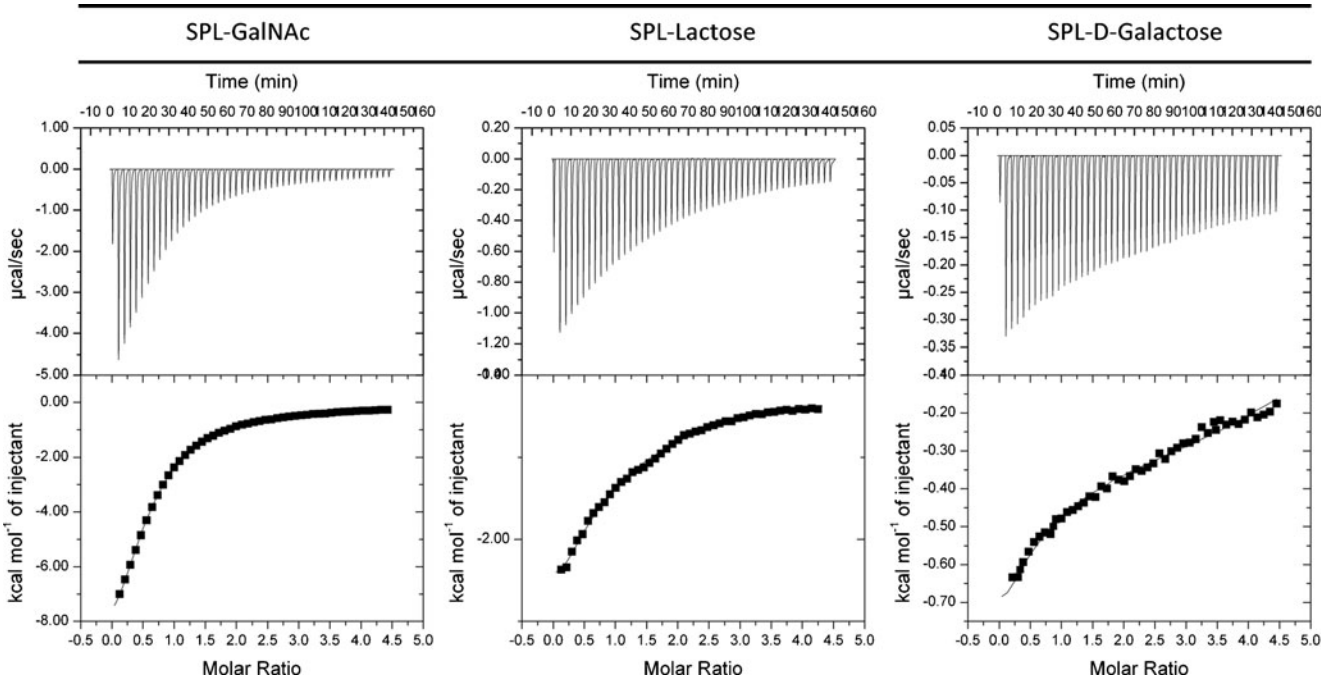

Fig. 3 Isothermal titration calorimetric analysis of GalNAc (**a**), lactose (**b**) and D-galactose (**c**) with native SPL. The *curve* represents the non-linear least-squares fit of the energy released as a function of the compounds added during the titration. Raw thermal power signal (*top*) and plot of integrated heat versus ligand/protein molar ratio (*bottom*)

pyranose ring of all sugars was bound at the same position in the native structure. They are able to make at least one hydrogen bond with any of the three residues, D88, A218 or S219. It might be assumed that the arrangement of sugars in the sugar binding region was in such a manner that the pyranose ring was placed first and the remaining portion of the sugars were aligned to get more interactions to strengthen the sugar-protein stability.

Apart from the above discussed three (D88, A218 or S219), the other residues that fell in the 4 Å radius of the pyranose ring atoms were also identified. They were A87, G106, T129, Y130, N132, G217 and L222. No common pattern of binding was shown when the native and DSAMD structures with the docked ligands were superimposed. However, a common nature was observed in the case of pyranose ring of most of the sugars. In the DSAMD structure a shift in the pyranose ring

Table 3 Thermodynamic parameters for the binding of sugars a) GalNAc b) lactose and c) D-galactose with native and demetallized SPL

	K	ΔH	ΔS	ΔG	Avg. ΔG
GalNAC GAL (Chi^2=218.2)					
Site 1	$2.92\times10^4\pm7.8\times10^2$	−898.9±27.5	17.4	−6.08	−6.08
Site 2	$3.4\times10^4\pm8.3\times10^2$	−647.9±100	18.1	−6.19	
Site 3	$2.54\times10^4\pm8.6\times10^2$	499.1±1.63	21.8	−6.00	
Site 4	$2.64\times10^4\pm6.5\times10^2$	−909.7±115	17.2	−6.03	
Lactose (Chi^2=862.6)					
Site 1	$1.56\times10^4\pm3.6\times10^2$	−3803±65.9	6.43	−5.72	−5.69
Site 2	$1.77\times10^4\pm4.7\times10^2$	−2302±272	11.7	−5.79	
Site 3	$1.37\times10^4\pm3.0\times10^2$	5356±524	36.9	−5.64	
Site 4	$1.28\times10^4\pm3.0\times10^2$	−5280±432	1.08	−5.60	
D-galactoese (Chi^2=418)					
Site 1	$1.30\times10^4\pm1.3\times10^2$	$-1.095\times10^4\pm46.9$	17.9	−5.61	−5.54
Site 2	$3.70\times10^3\pm44$	4487±337	33.4	−5.47	
Site 3	$9.11\times10^3\pm1.1\times10^2$	4494±713	33.2	−5.40	
Site 4	$1.44\times10^4\pm1.3\times10^2$	−6772±476	−3.68	−5.67	

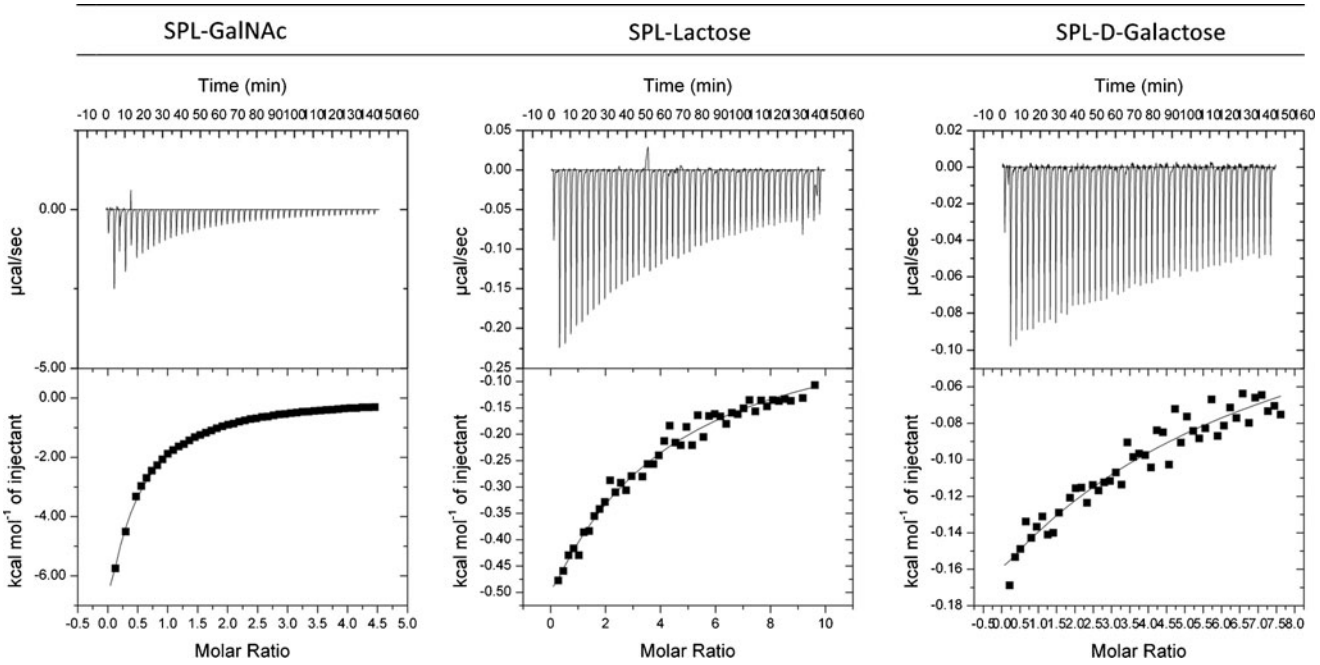

Fig. 4 Isothermal titration calorimetric analysis of GalNAc (**a**), lactose (**b**) and D-galactose (**c**) with demetallized SPL. The *curve* represents the non-linear least-squares fit of the energy released as a function of the compounds added during the titration. Raw thermal power signal (*top*) and plot of integrated heat versus ligand/protein molar ratio (*bottom*)

was observed, compared to the sugars bound in the native protein. The DSAMD structure explained that the sugar binding loop was shifted toward outside by making a new cavity, adjacent to the actual sugar binding cavity. It was also observed that the actual sugar binding cavity was compacted in both the monomers due to demetallization. Hence, the sugars could not bind in the sugar binding region as in the native structure. The binding mode of galactose in both native and demetallized structures are shown in Fig. 2. The interactions of the demetallized protein in solution might be similar to that of the modeled structure, showing drastic reduction in hemagglutination/sugar binding functions.

The results of ITC assays of GalNAc, lactose and D-galactose with SPL at 298.15 K and its corresponding parameters are shown in Fig. 3 and Table 3 respectively. Since SPL is a tetramer with one sugar binding site at each monomer, the ITC data were fitted using sequential binding mode with a stoichiometry n=4. The titrations were found to be exothermic in nature. The binding free energies of the sugar at the four sugar binding sites were calculated. On average, GalNAc (−6.08 kcal mol^{-1}) exhibit slightly higher binding free energy compared to lactose (−5.69 kcal mol^{-1}) and D-galacoste (−5.54 kcal mol^{-1}) (Table 2). These data agree with the earlier reported observation [10]. In the case of demetallized protein, the peaks were found to be exothermic. The ITC results also have good agreement among themselves and are also in agreement with the *in silico* predictions in terms of binding affinity (Table 3). The parameters are shown in Fig. 4. In the case of GalNAc, the final data could be fitted only after 5000 iterations. Hence, the error was found to be high in the fitted data. Similarly, for lactose and D-galactose the binding isotherms were also found to be improper and the data were found inappropriate for fitting. So it was concluded that the demetallization leads to the loss in conformational rigidity required for sugar binding specificity of the loop.

Conclusions

It might be assumed from the low hemagglutination score of the lectin for demetallized protein that it is due to the distortion of the loop region upon demetallization and consequent reduction in sugar binding affinity. There will be reduction in binding of blood cells onto the lectin molecule due to the weak binding of sugars of the surface glycoproteins of RBCs onto the lectin molecules, failing the formation of lectin:RBC-surface-sugar:lectin: network, leading to precipitation.

It was confirmed from the MD simulation studies that the metal ions are important for the structural stability as well as sugar binding property of SPL. The demetallization leads to large scale conformational changes in the metal binding loop. Since the sugar binding region is very close to the metal binding region, the perturbation in the loop affects the sugar binding as well. It was observed that the other secondary structure elements like sheets and helices were not deviated much since the hydrogen bonding network is strong. Also, no

highlighted changes due to metal chelation in the topology of SPL occurred even after 10 ns MD simulation. So, from these studies, it was concluded that the metal chelation is not affecting the quaternary structure of the lectin. However, it disables the sugar specificity and binding strength of the lectin. Also, a comprehensive analysis of the molecular docking and ITC data (Tables 2 and 3) suggests that the sugar specificity of the metal bound lectin and the loss of sugar specificity due to metal chelation are not linear.

Acknowledgments The authors acknowledge Bioinformatics Infrastructure facility (supported by Department of Biotechnology (DBT), Government of India) at the Department of Biotechnology and Microbiology, Kannur University and BIOGENE cluster of Bioinformatics Resources and Application Facility (BRAF) at Centre for Development of Advanced Computing (C-DAC) Pune, India for computational facilities. AJ thanks University Grants Commission (UGC) for a Junior Research Fellowship KVD thanks Indian Council of Medical Research (ICMR) for a Senior Research Fellowship.

References

1. Chandra NR, Kumar N, Jeyakani J, Singh DD, Gowda SB, Prathima MN (2006) Glycobiology 16:938–946
2. Jepson MA, Clark MA, Hirst BH (2004) Adv Drug Deliv Rev 56:511–525
3. Sharon N, Lis H (1989) Lectins. Chapman and Hall, London
4. Sharon N, Lis H (2004) Glycobiology 14:53–62
5. Nishi N, Shoji H, Seki M, Itoh A, Miyanaka H, Yuube K, Hirashima M, Nakamura T (2003) Glycobiology 13:755–763
6. Vijayan M, Chandra NR (1999) Curr Opin Struct Biol 9:707–714
7. Loris R, Hamelryck T, Bouckaert J, Wyns L (1998) Biochim Biophys Acta 1383:9–36
8. Lis H, Sharon N (1998) Chem Rev 98:637–674
9. Ohba H, Bakalova R, Moriwaki S, Nakamura O (2002) Cancer Lett 184:207–214
10. Geethanandan K, Abhilash J, Bharath SR, Sadasivan C, Haridas M (2011) Int J Biol Macromol 49:992–998
11. Mitra N, Srinivas VR, Ramya TN, Ahmad N, Reddy GB, Surolia A (2002) Biochemistry 41:9256–9263
12. Buts L, Dao-Thi MH, Loris R, Wyns L, Etzler M, Hamelryck T (2001) J Mol Biol 25:193–201
13. Dessen A, Gupta D, Sabesan S, Brewer CF, Sacchettini JC (1995) Biochemistry 34:4933–4942
14. Hamelryck TW, Dao-Thi MH, Poortmans F, Chrispeels MJ, Wyns L, Loris R (1996) J Biol Chem 271:20479–20485
15. Rabijns A, Verboven C, Rouge P, Barre A, Van Damme EJ, Peumans WJ, De Ranter CJ (2001) Proteins 44:470–478
16. Praveen K, Bernd N (2007) Biophys Chem 128:215–230
17. Ernesto CR, Raul GJ, Paulo MB (2002) J Mol Graph Model 21:227–230
18. Sandeep K, Debasisa M, Surolia A (2009) Biophys J 96:21–34
19. Naidoo KJ, Brady JW (1997) J Mol Struct (Theochem) 395-396: 469–475
20. Kaushik S, Mohanty D, Surolia A (2009) Biophys J 96:21–34
21. Thompson JD, Gibson TJ, Plewniak F, Jeanmougin F, Higgins DG (1997) Nucleic Acid Res 24:4876–4882
22. Cornell WD, Cieplak P, Bayly CI, Gould IR, Merz KM, Ferguson DM, Spellmeyer DC, Fox T, Caldwell JW, Kollman PA (1995) J Am Chem Soc 117:5179–5197
23. Jorgensen WL, Chandrasekhar J, Madura JD, Impeyand RW, Klein ML (1983) J Chem Phys 79:926–935
24. Accelrys Software Inc (2011) Discovery studio modeling environment, release 2.5. Accelrys Software Inc, San Diego
25. Scott WRP, Philippe HH, Ilario GT, Alan EM, Salomon RB, Jens F, Andrew ET, Thomas H, Peter K, Wilfred FVG (1999) J Phys Chem A 103: 3596–3607
26. Bouckaert J, Loris R, Poortmans F, Wyns L (1995) Crystallographic structure of metal-free concanavalin A at 2.5 Å resolution. Proteins 23:510–524